

Developing methods of using Digital Image Correlation for ice research

Waqas Ahmad, Malith Prasanna, Iman E Gharamti, Sven Bossuyt, Jukka Tuhkuri
Department of Mechanical Engineering, Aalto University, Espoo, Finland

ABSTRACT

This paper discusses the methods that have been developed to conduct ice fracture experiments with Digital Image Correlation (DIC). While conventional measurement methods provide information on ice response at specific locations, DIC provides full-field data at different areas of the specimen surface. Both test specimen in air and floating in a basin have been studied. The results show that DIC provides localized deformation zone information which could not be studied with conventional measurement techniques used in ice mechanics due to low spatial resolution.

KEY WORDS: Ice mechanics; Digital Image Correlation; Metrology

Introduction

Understanding of the deformation mechanisms of ice is important for design of safer and lighter offshore structures such as wind farms in ice covered sea areas. Ice exhibits brittle or ductile behavior depending on several parameters, including temperature and strain rate. (Schulson, 1999, 2001). Compared to other materials, ice is brittle at high homologous temperatures (Rist & Murrell, 1994). Significant work has been done to understand creep and plasticity of ice, as reviewed in (Schulson & Duval, 2009). As fracture significantly influences ice behavior, the transition between ductile and brittle failure of ice is important to understand. For example, high deformation rate interaction of ice floes and offshore structures can cause a combination of complex mechanical behaviors in ice, such as creep, tensile fracture, shear and rubble pileup. (Hallam et al., 1987; Wadhams, 1988).

Some of the methods use to measure ice deformation and crack propagation include strain gauges (Sinha, 1989), LVDTs (Gharamti et al., 2021b, 2021a), acoustic emission (Datt et al., 2020; Li & Du, 2016), electrical resistance method (ERM), and very high-speed photography (VHSP) (Arakawa et al., 1995; Arakawa & Petrenko, 2003; Gagnon, 2003; Parsons et al., 1987). All these methods differ from each other in their ability to provide details of the material deformation. For example, a strain gauge (or linear variable displacement transducer, LVDT) has limited spatial resolution as it provides information at a single point and requires physical contact with the specimen. Similarly, ERM requires physical contact with a specimen and fails to capture complex strain fields during deformation. Acoustic emission lacks strain distribution information and can only capture dynamic events such as crack propagation in a specimen. Lastly, for material such as ice, with small deformations compared to metals, if crack opening

is below pixel resolution, then the deformation cannot be captured using VHSP. These limitations can be resolved using full-field measurement techniques which provide higher spatial resolution and can capture different stages of a deformation. Figure 1 provides a summary of commonly used single-point and full-field displacement measurements techniques in experimental mechanics.

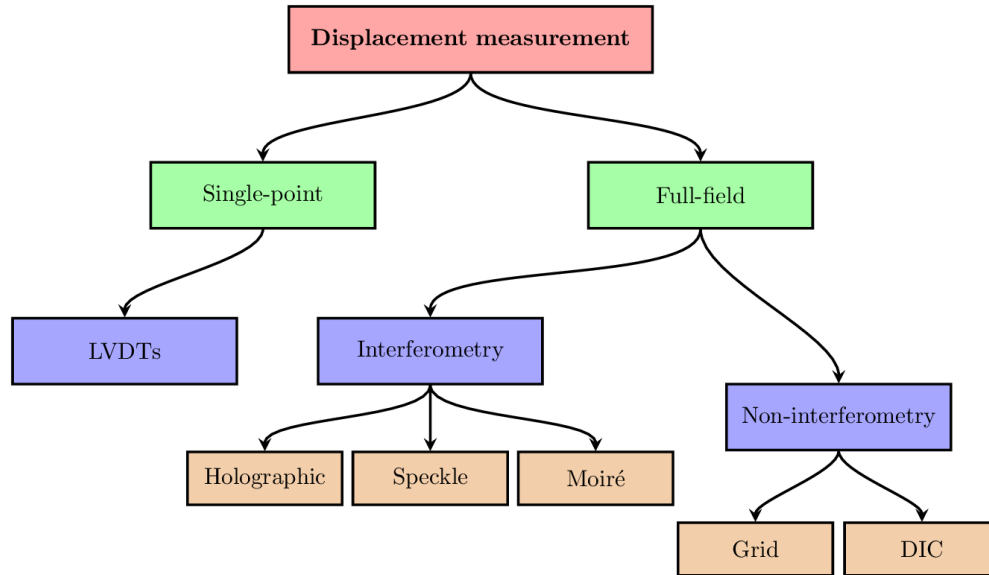


Figure 1: Different displacement measurement methods used in experimental mechanics. Most common method for displacement measurement in fracture studies of ice is using LVDTs.

Full-field displacement measurement techniques can be divided into interferometric and non-interferometric techniques. Interferometric techniques require a coherent light source to measure displacement of the specimen, but their accuracy is influenced by environmental effects. Hence, a vibration isolated platform is required to reduce uncertainty in displacement measurements (Bobroff, 1993). Phase difference between the undeformed and deformed specimen provides the displacements of the specimen. Non-interferometric full-field methods include grid method and Digital Image Correlation (DIC). Grid method extracts displacement information by calculating the phase shift of a regular and controlled grid (Grédiac et al., 2016). However, strict requirements of grid can become difficult to achieve if the specimen surface is rough. In comparison, DIC is based on template matching/tracking of speckle pattern on the surface of interest. Digital Image Correlation (DIC) has become a go-to technique in experimental solid mechanics. This is due to less stringent setup requirements.

The paper aims discuss the potential use of DIC in ice mechanics and outlines a method for achieving a sharp speckle pattern on ice surface. Moreover, two examples of DIC analysis of ice fracture experiments, one in air and another in an ice basin, are presented.

Principle of Digital Image Correlation

DIC is a non-contact full-field optical method that computes displacements and strains on a specimen surface using template matching/tracking (Peters & Ranson, 1982; Sutton et al., 1983). It compares gray scale pixel values of an undeformed (reference) image and deformed images. Image acquisition is done using digital cameras and images with sharp features can

increase the reliability of the results. DIC requires a speckle patterned surface to be captured with digital cameras. Image captured before loading is known as reference image and images captured during loading process are referred to as deformed images. As the deformations are calculated from image analysis, the principle of DIC remains the same irrespective of the image acquisition rate.

After capturing the reference image I_0 and a deformed image I_t at time instant t , the deformation can be calculated using the conservation of the optical flow equation:

$$I_0(\mathbf{x}) = I_t(\mathbf{x} + \mathbf{u}(\mathbf{x}, t)) + n(\mathbf{x}, t) \quad (1)$$

In Eq. 1, $\mathbf{u}(\mathbf{x}, t)$ is the displacement at pixel location \mathbf{x} at time t and $n(\mathbf{x}, t)$ is a random noise component cause by photon noise or digitization of pictures at the camera sensors. For the case of grey level conservation, the noise component disappears i.e., $n(\mathbf{x}, t) = 0$.

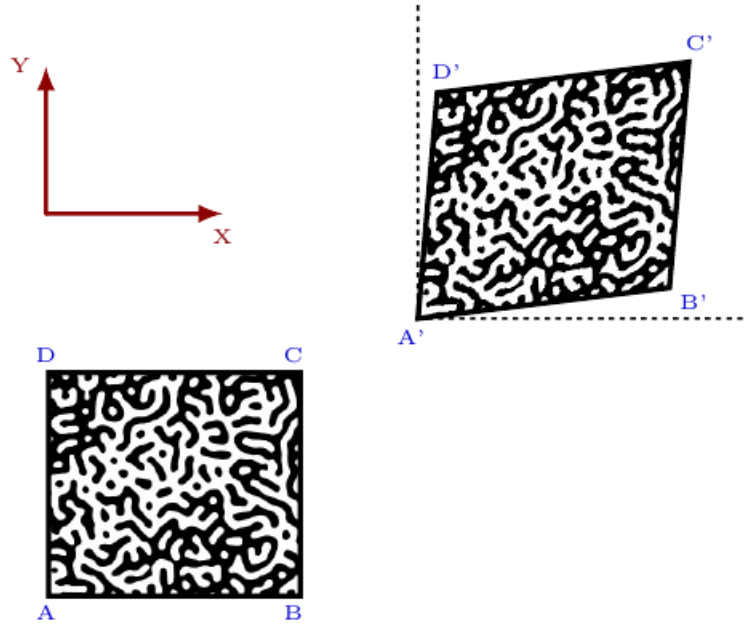


Figure 2: Deformation from I_0 reference image (ABCD) to $I_t(\mathbf{x} + \mathbf{u}(\mathbf{x}, t))$ deformed image A'B'C'D' at time instant t .

Displacement can be calculated by minimizing the functional \mathcal{R} in Eq. 2 with respect to degrees of freedom of required displacement field.

$$\mathcal{R}[\mathbf{u}] = \sum_{\Omega} [I_0(\mathbf{x}) - I_t(\mathbf{x} + \mathbf{u}(\mathbf{x}, t))]^2 \quad (2)$$

Only the grey scale values at the pixel location do not allow calculation of the displacement field therefore, the minimization problem is ill-posed. As a result, the correlation is done using a set of pixels rather than individual pixels. This set of pixels is commonly named as subset or

facet in DIC (Jones et al., 2018). Details of DIC algorithm are available in (Schreier et al., 2009).

As mentioned earlier, the deformation scale in ice is small compared to metals. Therefore, uncertainty quantification and precise estimation of error bounds in the measured displacements are key aspects for future potential of DIC in ice mechanics. Variation in the camera setup and quality of the speckle pattern cause differences in measurement uncertainty between experiments. Figure 3 shows various errors sources that contribute to the uncertainty in DIC measurements (Reu, 2013).

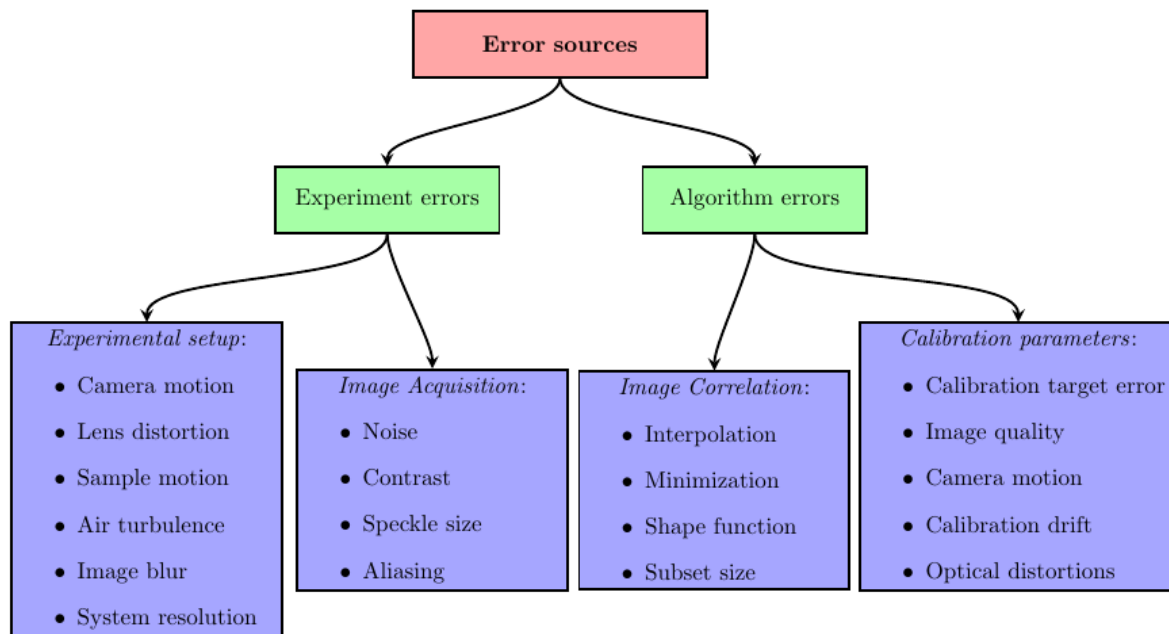


Figure 3: Experiment and algorithm errors that result in defining error bounds of DIC measurements

As the algorithm errors are specific to the DIC software used for the analysis, we focus on the experiment errors with emphasis on reducing camera/sample motion and speckle patterns errors for use in fracture experiments with floating ice specimen.

A method to achieve reliable speckle pattern on ice

Two sets of experiments are discussed below: Mode-I fracture of saline ice by using semi-circular bending (SCB) specimens in a cold room, and mode-I fracture of edge-cracked rectangular plate (ECRP) specimens with floating freshwater ice at the Aalto Ice and Wave Tank. **Error! Reference source not found.** shows the experimental setup for both set of experiments along with the region of interest (ROI) that was stamped with a speckle pattern for DIC.

Since the ice surface in both experiments was not smooth, a sander was used to smoothen the ROI to achieve uniform speckle pattern. Before stamping the surfaces, an initial crack was made on each specimen. A thin layer of TiO_2 solution was brushed on the smoothened surface

to achieve maximum contrast with the black speckle pattern. Carbon powder was mixed with corn starch to make black pattern ink. Corn starch prevented sharp pattern features from fading after stamping the ice. Finally, the crack tip was sharpened by using a 0.4 mm thick blade for the saline ice experiments and a 0.5 mm thick blade for the freshwater ice experiments. Specimens were loaded based and the surface deformations around the initial crack were captured by using a stereo-DIC system. Analysis of the digital images was done using software VIC-3D, by Correlated Solutions. Test parameters, specimen details, and DIC setup for both the freshwater and saline ice experiments are listed in Table 1.

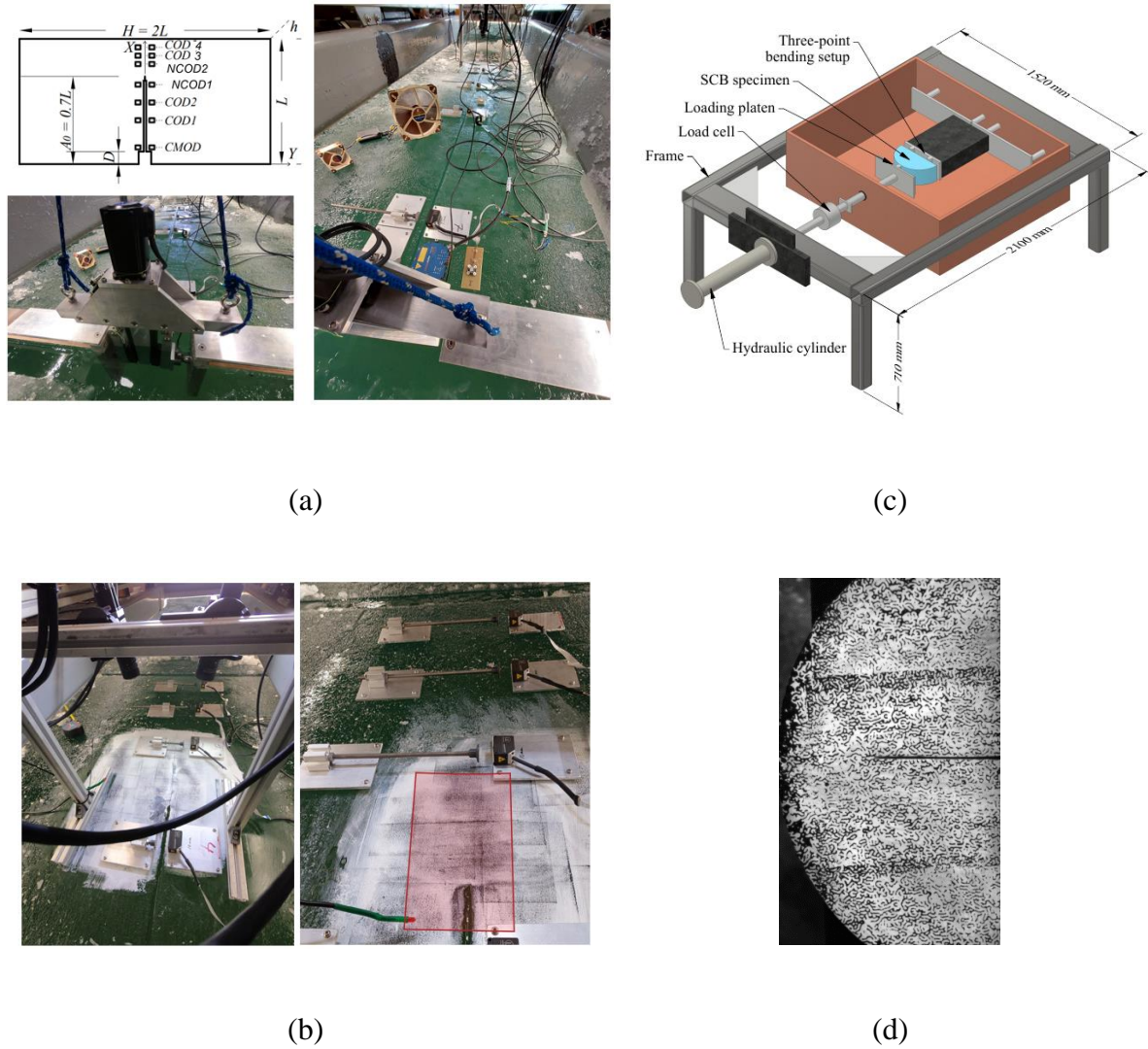


Figure 4: Experimental setup and stamped DIC pattern for: (a,b) floating freshwater ice specimens and (c,d) saline ice experiments

Table 1: Details of the experiment types and specimens used to study ice fracture using DIC.

| Parameters | Saline Ice | Freshwater Ice |
|-----------------------------------|------------------------------------|---|
| Experiment type | Dry, in air | Wet, floating in water |
| Specimen geometry | Semi-circular bending | Edge-cracked rectangular plate |
| Loading configuration | Load-controlled | Displacement controlled |
| Specimen size | 183, 360, and 596 mm (Diameter) | 3x6 m |
| Stereo-DIC camera system location | Isolated from testing setup | Camera mounting system placed on floating ice sheet |

For floating freshwater ice experiments, the camera system was placed on the ice sheet itself to prevent any effect of rigid body motion, although this can be removed from DIC displacements. However, this helped also in isolating any external vibrations. Moreover, by placing the camera system on the ice sheet, the limitation of specimen size was removed, and the camera mounting system was significantly simplified. This potentially paves way for future field experiments where much larger specimens can be tested.

RESULTS AND DISCUSSION

As the DIC involves analysis of digital images, a frame with damage/crack travelling through a complete ROI can be used to mark critical regions e.g., region ahead of crack tip, and observe the damage development during different phases of the experiment. Using a similar approach, crack path can be extracted using cross-correlation of displacement field and discontinuity function (Ahmad et al., 2022). Figure 5 shows examples of percentage strain ϵ_{yy} and displacement V normal to the crack propagation direction.

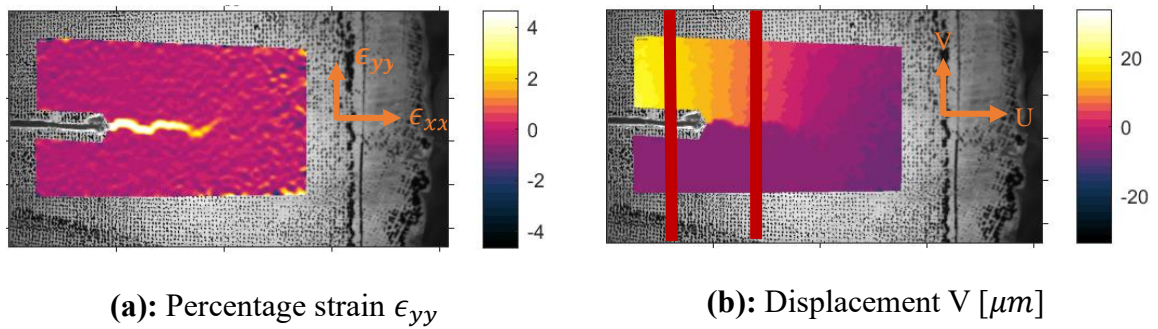


Figure 5: Percentage strain ϵ_{yy} and V displacement normal to the crack propagation direction for SCB specimen. Every column in ROI serves as virtual LVDT which can be used to calculate crack opening displacement. Red lines in V displacement depict two such virtual LVDTs.

The effect of contact between the loading device and the ice specimen in the semi-circular bending specimens can also be observed from the localized deformation at these points to see

effectiveness of SCB specimens. Figure 6(a) shows a case in which significant damage was observed at the loading point before final failure. The size of this damage zone can help to estimate the specimen sizes where the crack tip is far enough from the crack tip to prevent influence of the contact damage to the crack tip.

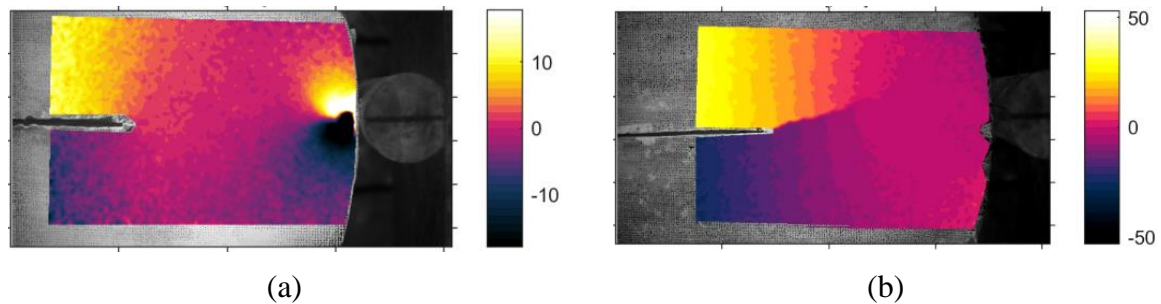


Figure 6: V displacement of contact between loading device and saline ice SCB specimen. (a) shows significant damage at the contact point with no observable damage at the crack tip whereas (b) shows crack growth observable at the displacement field with no damage at the contact point.

CONCLUSIONS

This study presents DIC as a potential measurement technique to study ice behavior under different loading conditions. Moreover, a method of obtaining robust speckle pattern with sharp features is also discussed. Since the technique was successfully demonstrated on floating ice sheets, the work also paves way for using the method in future field experiments. For the field experiments, the speckle pattern can be stamped before the specimen geometry is cut. The high spatial resolution data obtained with DIC can help us better understand the mechanical behavior of ice. Due to large grain size of ice compared to metals, it is possible to conduct full-field studies at the grain level too. For this, the speckle pattern size needs to be adjusted accordingly. Accuracy of the measurement varies with the quality of the speckle pattern. For this study, the error bounds generally lied between $\pm 3 \mu m$.

ACKNOWLEDGEMENTS

Author is grateful to Finnish Maritime foundation, Merenkulun säätiö, for funding this research.

REFERENCES

- Ahmad, W., Prasanna, M., Bossuyt, S., & Tuhkuri, J. (2022). Measurement of crack speed in S2 saline ice using Digital Image Correlation. *26th IAHR International Symposium on Ice*.
- Arakawa, M., Maeno, N., & Higa, M. (1995). Direct observations of growing cracks in ice. *Journal of Geophysical Research*, *100*(E4). <https://doi.org/10.1029/95je00278>
- Arakawa, M., & Petrenko, V. F. (2003). Observation of crack propagation in saline ice and freshwater ice with fluid inclusion. *Canadian Journal of Physics*, *81*(1–2). <https://doi.org/10.1139/p03-021>

- Bobroff, N. (1993). Recent advances in displacement measuring interferometry. *Measurement Science and Technology*, 4(9). <https://doi.org/10.1088/0957-0233/4/9/001>
- Datt, P., Chandel, C., Kumar, V., Sheoran, R., Nasker, D., Kapil, J. C., & Srivastava, P. K. (2020). Analysis of acoustic emission characteristics of ice under three-point bending. *Cold Regions Science and Technology*, 174. <https://doi.org/10.1016/j.coldregions.2020.103063>
- Gagnon, R. (2003). High-speed video analysis of fracture propagation in a thick-edge-loaded freshwater ice sheet. *Canadian Journal of Physics*, 81(1–2). <https://doi.org/10.1139/p02-134>
- Gharamti, I. E., Dempsey, J. P., Polojärvi, A., & Tuhkuri, J. (2021a). Creep and fracture of warm columnar freshwater ice. *Cryosphere*, 15(5). <https://doi.org/10.5194/tc-15-2401-2021>
- Gharamti, I. E., Dempsey, J. P., Polojärvi, A., & Tuhkuri, J. (2021b). Fracture energy of columnar freshwater ice: Influence of loading type, loading rate and size. *Materialia*, 20. <https://doi.org/10.1016/j.mtla.2021.101188>
- Grédiac, M., Sur, F., & Blaysat, B. (2016). The Grid Method for In-plane Displacement and Strain Measurement: A Review and Analysis. *Strain*, 52(3). <https://doi.org/10.1111/str.12182>
- Hallam, S. D., Duval, P., & Ashby, M. F. (1987). STUDY OF CRACKS IN POLYCRYSTALLINE ICE UNDER UNIAXIAL COMPRESSION. *Journal de Physique (Paris), Colloque*, 48(3). <https://doi.org/10.1051/jphyscol:1987143>
- Jones, E. M. C., Iadicola, M. A., Bigger, R., Blaysat, B., Boo, C., Grewer, M., Hu, J., Jones, A., Klein, M., Raghavan, K., Reu, P., Schmidt, T., Siebert, T., Simenson, M., Turner, D., Vieira, A., & Weikert, T. (2018). A Good Practices Guide for Digital Image Correlation. In *International Digital Image Correlation Society*.
- Li, D., & Du, F. (2016). Monitoring and evaluating the failure behavior of ice structure using the acoustic emission technique. *Cold Regions Science and Technology*, 129. <https://doi.org/10.1016/j.coldregions.2016.06.003>
- Parsons, B. L., Snellen, J. B., & Hill, B. (1987). Preliminary measurements of terminal crack velocity in ice. *Cold Regions Science and Technology*, 13(3). [https://doi.org/10.1016/0165-232X\(87\)90004-8](https://doi.org/10.1016/0165-232X(87)90004-8)
- Peters, W. H., & Ranson, W. F. (1982). Digital Imaging Techniques In Experimental Stress Analysis. *Optical Engineering*, 21(3). <https://doi.org/10.1117/12.7972925>
- Reu, P. L. (2013). Uncertainty quantification for 3D digital image correlation. *Conference Proceedings of the Society for Experimental Mechanics Series*, 3. https://doi.org/10.1007/978-1-4614-4235-6_43
- Rist, M. A., & Murrell, S. A. F. (1994). Ice triaxial deformation and fracture. *Journal of Glaciology*, 40(135), 305–318. <https://doi.org/10.3189/S0022143000007395>
- Schreier, H., Orteu, J. J., & Sutton, M. A. (2009). Image correlation for shape, motion and deformation measurements: Basic concepts, theory and applications. In *Image Correlation for Shape, Motion and Deformation Measurements: Basic Concepts, Theory and Applications*. <https://doi.org/10.1007/978-0-387-78747-3>
- Schulson, E. M. (1999). The Structure and Mechanical Behavior of Ice. *JOM*, 51(2). <https://doi.org/10.1007/s11837-999-0206-4>

- Schulson, E. M. (2001). Brittle failure of ice. *Engineering Fracture Mechanics*, 68(17–18).
[https://doi.org/10.1016/S0013-7944\(01\)00037-6](https://doi.org/10.1016/S0013-7944(01)00037-6)
- Schulson, E. M., & Duval, P. (2009). Creep and fracture of ice. In *Creep and Fracture of Ice* (Vol. 9780521806206). <https://doi.org/10.1017/CBO9780511581397>
- Sinha, N. K. (1989). Use of foil strain gauges in ice over a wide loading rate. *Cold Regions Science and Technology*, 16(2). [https://doi.org/10.1016/0165-232X\(89\)90015-3](https://doi.org/10.1016/0165-232X(89)90015-3)
- Sutton, M., Wolters, W., Peters, W., Ranson, W., & McNeill, S. (1983). Determination of displacements using an improved digital correlation method. *Image and Vision Computing*, 1(3). [https://doi.org/10.1016/0262-8856\(83\)90064-1](https://doi.org/10.1016/0262-8856(83)90064-1)
- Wadhams, P. (1988). *Ice Mechanics - Ice Mechanics: Risks to Offshore Structures*. T. J. O. Sanderson 1988. London, Graham and Trotman. 253 p.
<https://doi.org/10.1017/s0032247400009712>